Chapter 1

The Organic Set of NMR Spectra

There are six NMR spectral methods, which are usually first measured on a routine basis if an organic chemist has produced a new compound. Usually, this organic set is sufficient for a complete structural elucidation, especially if additional support comes from mass spectrometry and IR- or UV-spectroscopy.

These six methods are:

We describe therefore in this first chapter these six methods in some detail using strychnine as an example. Strychnine with its rather complicated molecular structure provides all the typical problems encountered during spectral assignments in organic chemistry. With concurrent instrumentation and about 20 mg of substance having a molecular weight around 500 Da, the total recording time of these techniques will be about 5 h.

Of course, this book offers much more, but this organic set comprises the most essential of all our essentials.

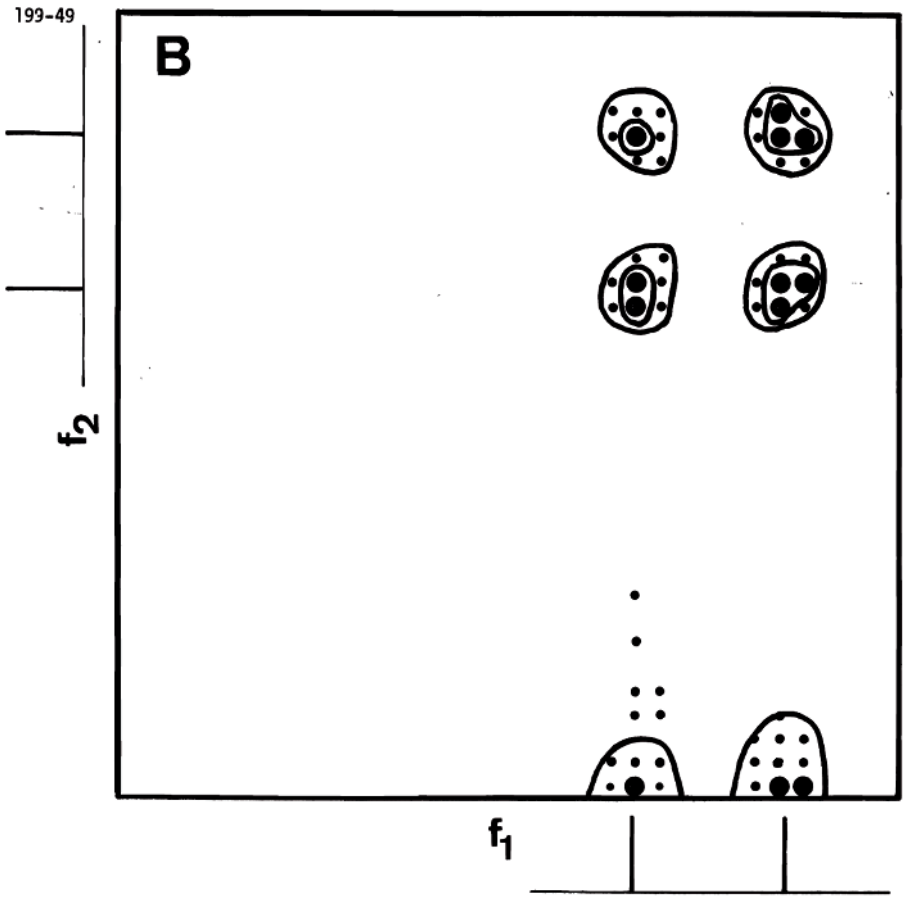

These spectra are preliminary in several respects. First of all, resolution is severely limited by the available computer memory. A 64x64 data matrix was used. Secondly, the absolute value of the 2D spectrum is plotted disregarding phase information which may be of particular interest. This experiment has several further interesting aspects which we presently are investigating.

Sincerely yours

Richard

Richard R. Ernst

taken from *TAMU NMR Letters*, **1975,** *199*, 49.

Experiment 1.1

^1H NMR Experiment

1. Purpose

The aim of the standard ^1H NMR experiment is to record a routine proton NMR spectrum in order to get structure-related information for the protons of the sample, i. e. chemical shifts, spin–spin couplings, and intensities. Here we apply this standard procedure to strychnine and discuss different weighting functions and problems of integration.

The prospect of measuring very rapid reaction rates by NMR provided the inspiration for getting an affirmative response from Linus Pauling [then chairman of the division of Chemistry and Chemical Engineering at California Institute of Technology] that "with NMR, we could investigate the borderline between resonance and tautomerism". For example, investigating the NMR spectrum of cycloheptatriene with temperature to see if it existed as a rapidly equilibrating mixture of cycloheptatriene and norcaradiene, or was what later would be called a "monohomobenzene". The argument was persuasive and we soon ordered a 30-MHz Varian proton and fluorine spectrometer.

J. D. Roberts, * 1918 "A Personal NMR Odyssey" *Enyclopedia of NMR*, **1996**, *1*, 590–598.

2. Variants

Variants of this form of NMR spectroscopy include first of all excitation with different pulse angles.

However, since recent NMR instruments are sensitive enough, usually one 90° scan is sufficient to obtain a spectrum. Therefore no considerations about reduced pulse angles are necessary. Second, if a strong solvent signal is present, different forms of signal suppression are available. These are discussed in chapter 3.

3. Pulse Scheme and Phase Cycle

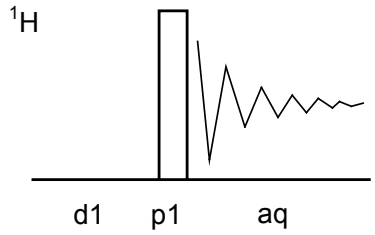

p1: x, x, -x, -x, y, y, -y, -y
aq: x, x, -x, -x, y, y, -y, -y

Scheme 1.1-1

4. Acquisition

Special values used for the spectrum shown:

Sample: 3% strychnine in $CDCl_3$.
Time requirement: 1 min
Spectrometer: Bruker DRX-600 with 5-mm-TBI-probe

td:	64K
sw:	15 ppm
aq:	3.6 s
o1:	middle of ^1H NMR spectrum
d1:	2 s
ns:	1

These data will lead to an FID digital resolution of 0.28 Hz/point for the real or imaginary part of the FID.

Common values:

p1: 90° ^1H transmitter pulse
d1: relaxation delay

The appearance of an unsplit methyl signal in a CH_3CH moiety, where the chemical shift difference was large compared to the vicinal coupling constant, expected to be about 7 Hz, subsequently impressed on me the importance of MR spectral analysis. When I understood what was going on, I wrote a paper which was published in 1961 on the nature of the signals of C-methyl groups, and this explained many anomalous "coupling constants" involving methyl groups in steroids and other compounds; it anticipated later research by others on virtual coupling. Although spectral analysis is becoming almost a lost art in the midst of so-called "modern NMR", it is in fact just as useful and necessary as it has ever been, in my own experience.

F. A. L. Anet, * 1926 "A lapsed organic chemist in the wonderland of NMR" *Enyclopedia of NMR*, **1996**, *1*, 187–190.

5. Processing

Use zero filling to si = 64K and exponential weighting with lb = 0.1 Hz, phase correction and referencing to internal TMS, which is the only acceptable reference scheme. The digital resolution of the spectrum will be with these data sw/si = 0.14 Hz/point. Before integration, perform phase and baseline correction on the spectrum accurately. A comparison of the spectra in Fig. 1.1-3 and 1.1-4 shows how a Gaussian weighting function with lb = –1 Hz and gb = 0.3 makes additional small spin couplings visible.

6. Result

The figures show two expansions of the 600 MHz ^{1}H NMR spectrum of strychnine.

A closer inspection of the integrals reveals that the integral of H-4 is too small as compared to all other integrals of the compound. Although the spectrum was recorded with only one scan, the waiting time after the receiver gain adjust command before and the actual measurement was appartently too short (see Question A).

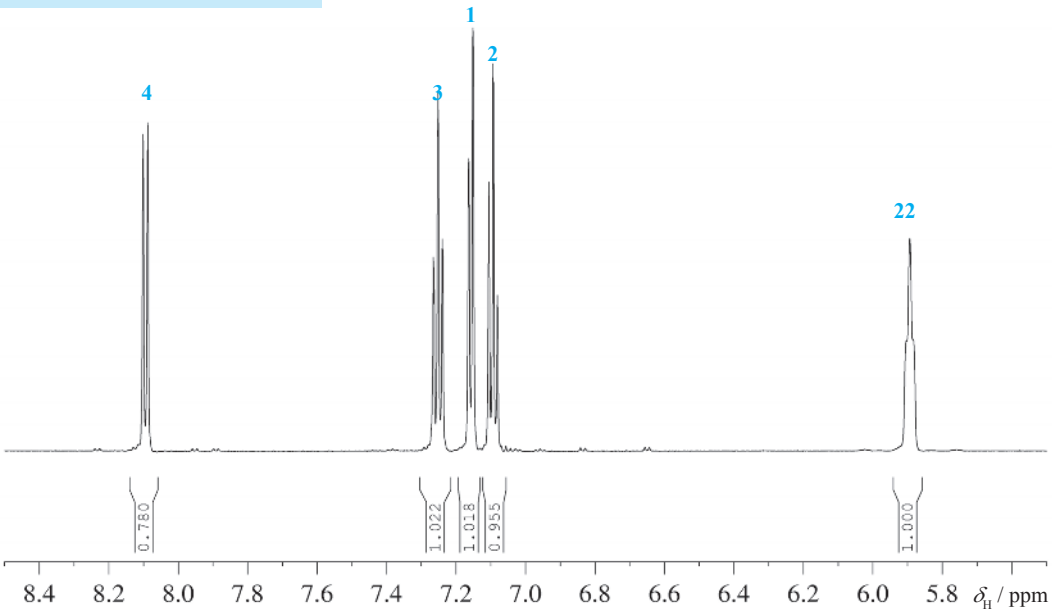

Fig. 1.1-1 Expansion of the ^{1}H-NMR spectrum in the aromatic region

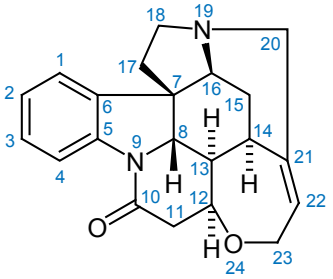

Scheme 1.1-2

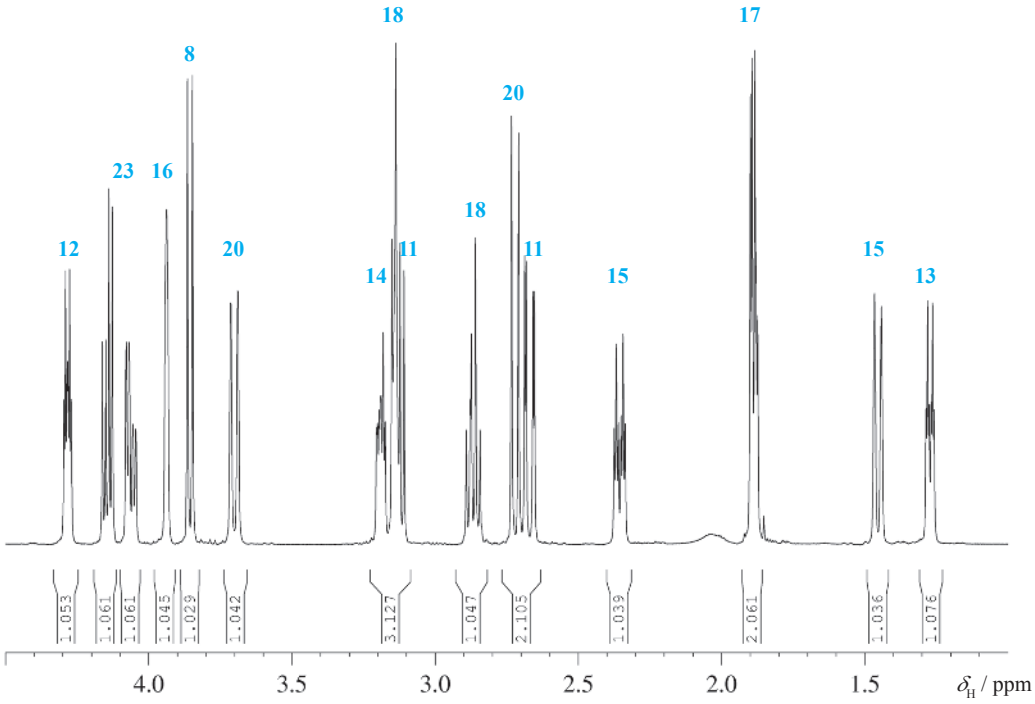

Fig. 1.1-2 Expansion of the ^{1}H-NMR spectrum in the aliphatic region

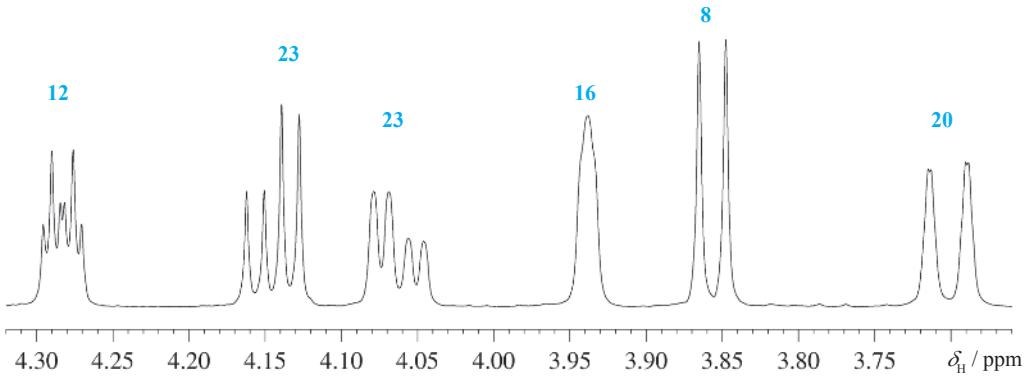

Fig. 1.1-3 Edited with lb = 0.1 Hz (zoom of Fig. 1.1-2)

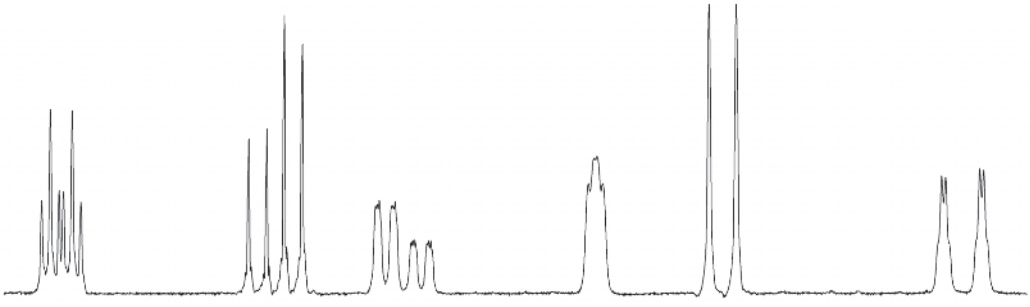

Fig. 1.1-4 Edited with gb = 0.3, lb = –1

7. Comments

The excitation pulse p1 converts the equilibrium magnetization of the ^1H nuclei into a transverse magnetization as shown in Equation (1). During the acquisition time chemical shifts and spin–spin couplings develop in the *x,y* plane, as shown separately in Equations (2) and (3), and are detected by the receiver in the *x,y* plane in quadrature mode.

(1)

$$I_{H_z} \xrightarrow{90^\circ I_x} -I_{H_y}$$

(2)

$$-I_{H_y} \xrightarrow{\Omega I_z t} -I_{H_y}\cos\Omega t + I_{H_x}\sin\Omega t$$

(3)

$$-I_{H_y} \xrightarrow{\pi J\, 2I_{1z}I_{2z}\, t} -I_{H_y}\cos\pi Jt + 2I_{H_x}I_{H_z}\sin\pi J\, t$$

[1] T. D. W. Claridge, "High-resolution NMR techniques in organic chemistry", Pergamon, Oxford, **1999**.

[2] I. K. M. Sanders, B. K. Hunter, "Modern NMR spectroscopy", 2nd Edition, Oxford University Press, Oxford, **1993**.

[3] H. Friebolin, "Basic one- and two-dimensional NMR spectroscopy", 3rd Edition, Wiley-VCH, Weinheim, **1998**.

[4] H. Günther, "NMR Spectroscopy", 2nd Edition, Wiley, Chichester, **1995**.

8. Questions

A. Suggest a reason why the integral of H-4 is considerable smaller than the others.

B. How would one classify the aromatic spin system?

C. The intensity pattern of the signals between 4.2 and 4.0 ppm has a special name?

D. The signals at 2.35 and 1.27 ppm both belong to the methylene group of C-15 and are spin coupled to each other; however, only one has an additional spin coupling. Why?

9. Own Observations

Experiment 1.2

ATP-^{13}C NMR

1. Purpose

The aim of a routine ^{13}C NMR experiment is to record a ^{13}C NMR spectrum with proton broad-band decoupling and data accumulation in order to get chemical shift information for structure determination. At the same time one wants to have multiplicity information. From the many schemes proposed we feel the APT (**A**ttached **P**roton **T**est) technique is the most useful and convenient method available, especially if carried out with a chirp 180° pulse on the carbon channel to avoid phase problems at high field spectrometers.

2. Variants

Alternative methods that give information about the multiplicities are INEPT, DEPT, DEPTQ, and PENDANT, and the historic off-resonance ^{1}H-decoupling technique. Unlike INEPT or DEPT, the APT method yields ^{13}C NMR spectra that are only enhanced by the NOE. However, APT also gives information about quaternary carbon atoms. Improved modifications of APT are known [2-4].

3. Pulse Scheme and Phase Cycle

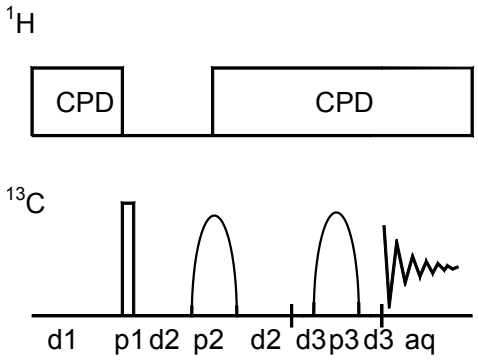

p1: $(x)_4$, $(y)_4$, $(-x)_4$, $(-y)_4$

p2: x, y, -x, -y, y, -x, -y, x, -x, -y, x, y, -y, x, y, -x

p3: x, y, y, x, $(y, x, x, y)_2$, x, y, y, x

aq: x, x, -x, -x, y, y, -y, -y

Scheme 1.2-1

4. Acquisition

Special values used for the spectrum shown:

Sample:	3 % strychnine in $CDCl_3$.
Time requirement:	1 h
Spectrometer:	Bruker DRX-600 with 5-mm TBI probe

Fig. 1.2-1 P. J. Lauterbur (1929-2007)

Common values:

p1: 45° ^{13}C transmitter pulse
p2: 180° ^{13}C CHIRP pulse
d1: relaxation delay
d2: $1/J_{CH}$
d3: switching delay
CPD composite pulse decoupling

Fig. 1.2-2 J. D. Roberts (*1918)

Natural-abundance ^{13}C NMR was not really routine until the introduction of broadband noise proton decoupling. Such decoupling removes the proton splittings from the ^{13}C resonances and, in addition, gives a favorable nuclear Overhauser effect (NOE). Thus, a proton-coupled doublet ^{13}C resonance, such as exhibited by trichloromethane, with broadband decoupling produces a singlet peak with a sixfold increase over the intensity of each of the individual doublets. There is hardly a better early example of the utility of broadband proton decoupling for ^{13}C spectra than for cholesterol. Weigert had found it impossible to make sense out of the 15-MHz coupled spectrum of cholesterol, because of the jumble of resonances and the generally poor signal-to-noise ratio, even after hours of signal averaging. In contrast, with broadband proton decoupling, 25 rather well-separated resonances were observed. A challenge was thus presented of spectral assignments and was met by H. Reich and M. Jautelat in about six months. An important element in the unraveling of the resonances was D. M. Grant's work on the steric influence of axial methyl groups on ^{13}C shifts in cyclohexane rings.

J. D. Roberts, * 1918 "A personal NMR odyssey" *Enyclopedia of NMR*, **1996**, *1*, 590-598.

td: 64K
sw: 200 ppm
aq: 1.0 s
p1: 45° ^{13}C transmitter pulse 6 µs
o1: middle of ^{13}C NMR spectrum
o2: middle of ^{1}H NMR spectrum
p2: adiabatic chirped 180° ^{13}C pulse [crp 60, 0.5, 20.1; 500 µs, 5.5 dB]
d1: 2 s
d2: 6.9 ms corresponding to a J_{CH} = 145 Hz
d3: 100 µs
CPD: WALTZ16 sequence, individual 90° ^{1}H pulse:100 µs at 12 dB
ns = 1024

5. Processing

Use zero filling to si = 64K and exponential weighting with lb = 2 Hz, phase correction and referencing to either internal TMS or via the Ξ scale using the proton spectrum of the same sample.

6. Result

The figure shows the ^{1}H broad-band decoupled APT ^{13}C NMR spectrum of strychnine as obtained on an DRX-600 spectrometer using a TBI probe head. Because of the inverse probe a certain number of scans had to be accumulated. Note that as usual no integration is performed, since under routine conditions the signal areas are not necessarily proportional to the number of ^{13}C nuclei giving rise to that signal. Furthermore, since the d2 delay hits exactly one $J_{C,H}$ value, the others will be scaled in intensity.

The signal of the solvent $CDCl_3$ was adjusted to be negative like the other signals of carbon atoms carrying no protons. Signals of CH and CH_3 groups are positive and signals of CH_2 groups negative.

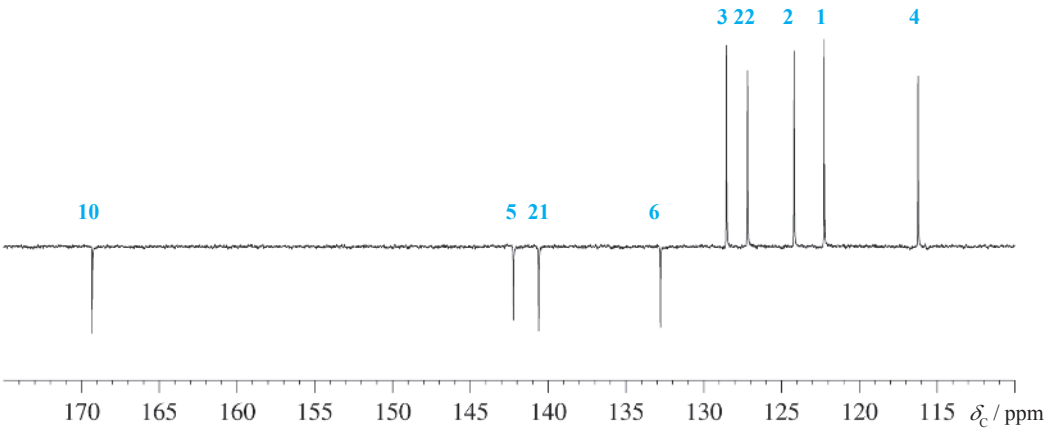

Fig. 1.2-3 Expansion of the ^{13}C NMR spectrum in the aromatic and carbonyl region

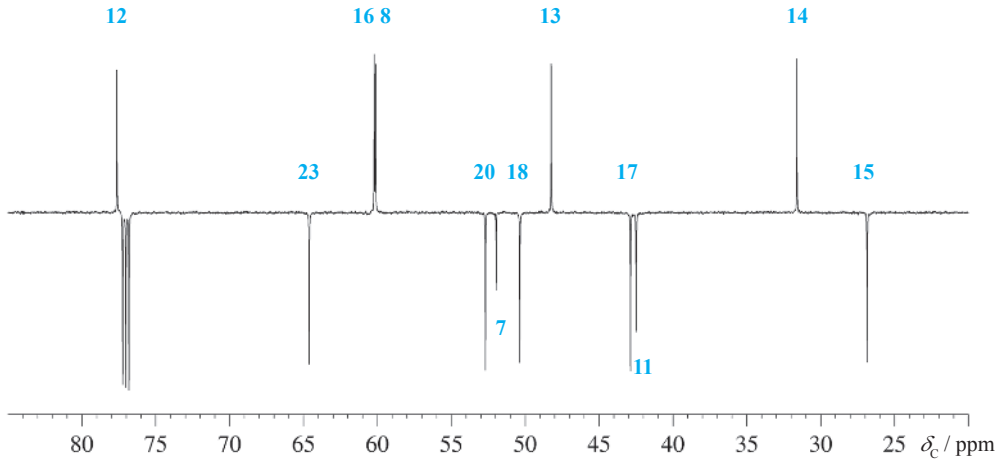

Fig. 1.2-4 Expansion of the ^{13}C NMR spectrum in the aliphatic region

7. Comments

The APT sequence is in principle a double spin-echo experiment. In the first echo period d2 the evolution of *J*-coupling modulates the phases of the signals according to C_q or CH_2 groups respective CH and CH_3 groups. By using a 45° or shorter excitation pulse a part of the initial magnetization remains in the *z*-direction and is inverted to $-z$ by the first 180° pulse. This could lead to a canceling of signals with long spin-lattice relaxation times, but in the second spin-echo period the 180° pulse reinverts the *z*-magnetization, thus eliminating this problem. In comparison with all other editing techniques APT still seems to be the most simple and efficient method, since it gives in one experiment all the necessary information on *all* sorts of carbon atoms. The lower sensitivity compared with polarization transfer methods such as DEPT is in practice not important for the C,H spin pair. See, however, the new DEPTQ experiment where the shortcomings of the traditional DEPT are overcome.

Scheme 1.2-2

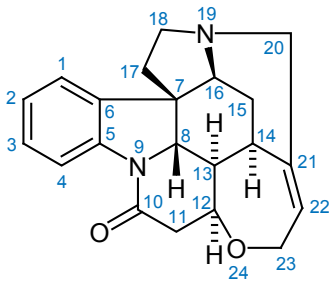

It was the time of the Korean War, however, and my deferments ran out. I was drafted and eventually ended up at the Army Chemical Center. where my 'experience' with NMR got me a transfer and assignment to help set up the Varian NMR machine (40 MHz proton and ^{19}F, 17 MHz ^{31}P) which they purchased to support chemical warfare research. There I actually learned something about NMR and even published a few papers. After Army service two options developed: go to Illinois as a graduate student with Gutowsky, or persuade the Mellon Institute to buy an NMR spectrometer. The institute itself declined, but the Dow Corning group took the plunge, at least partly because I claimed that useful ^{29}Si spectra would be possible. I chose that option, visited Varian, and confirmed that ^{29}Si spectra could be seen (with an 8.5 Mc s^{-1} rf unit) and immediately decided that ^{13}C would be even more interesting. I soon published the first paper on ^{13}C NMR spectra. The rest is another branch of personal and scientific history, except that ^{13}C led to interest in spin decoupling and biological polymers, which were both to become essential links in the chain of events leading to 'zeugmatography', as I originally called magnetic resonance imaging.

Paul Lauterbur (1929-2007)
"One Path out of Many – How MRI actually began" *Enyclopedia of NMR*, **1996**, *1*, 445–449.

[1] H.-O. Kalinowski, S. Berger, S. Braun, "Carbon-13 NMR spectroscopy", Wiley, Chichester, **1988**.

[2] T. D. W. Claridge, "High-resolution NMR techniques in organic chemistry", Pergamon, Oxford, **1999**.

[3] K. M. Sanders, B. K. Hunter, "Modern NMR spectroscopy", 2nd Edition, Oxford University Press, Oxford, **1993**.

[4] S. L. Patt, J. N. Shoolery "Attached proton test for carbon-13 NMR" *J. Magn. Reson*. **1982**, *46*, 535–539.

[5] J. C. Madsen, H. Bildsøe, H. J. Jakobsen, O. W. Sørensen "ESCORT editing. An update of the APT experiment" *J. Magn. Reson*. **1986**, *67*, 243–257.

[6] A. M. Torres, T. T. Nakashima, R. E. D. McClung "Improved *J*-compensated APT experiments" *J. Magn. Reson*. Ser. A **1993**, *101*, 285–294.

[7] U. Beckmann, W. Dietrich, R. Radeglia "ORSAT and modifications of SEFT and APT" *J. Magn. Reson.* **1999**, *137*, 132–137.

8. Questions

A. What is understood by the "Ernst angle"?

B. Which parameter controls the correct phases obtained in this experiment?

C. What is meant with a WALTZ16 sequence?

D. The signals of $CDCl_3$ show a 1:1:1 triplet with a spin coupling of 31.7 Hz. Explain and calculate from this the spin coupling found in $CHCl_3$.

E. Looking at the spectrum and the chemical formula of strychnine, you should be able to assign at once at least two carbon atoms. Which ones?

9. Own Observations

Experiment 1.3

COSY

1. Purpose

The COSY (**CO**rrelation **S**pectroscop**Y**) pulse sequence generates a 2D NMR spectrum in which the signals of a normal ^{1}H NMR spectrum are correlated with each other. Cross-peaks appear if homonuclear spin coupling is present; thus the COSY sequence detects coupled pairs of protons (or pairs of other nuclei such as ^{19}F, ^{31}P or even ^{13}C in the case of labelled proteins). Since coupled protons are usually separated by two or three bonds, the connectivity and very often a chemical structure can be derived from the COSY spectrum; however, one must be also aware of long-range spin couplings. The COSY sequence is the most important and most frequently used 2D NMR experiment.

2. Variants

Due to the importance of the COSY technique an impressive number of variants has been developed in the last 40 years. The current Bruker pulse sequence library, for example, contains more than 30 different applications, and it is impossible to discuss them all in this book. We show here a COSY sequence which includes a gradient-selected double quantum filter and the echo-antiecho scheme for the phase sensitive frequency generation in the indirect dimension. The reason for this selection is that in COSY one usually wants to see and interpret the interaction of two protons with each other. The double quantum filter suppresses singlets and reduces multiplets to AX patterns; the echo-antiecho scheme provides phase sensitive spectra.

Other important variants of COSY which should be mentionend are:

(1) The long-range COSY, which emphasizes connectivities caused by small spin-coupling constants. This is important in the case of allylic or W-spin couplings < 2 Hz.

(2) The COSY-45 or the E.COSY methods, which lead to slim diagonals and allow the determination of the sign of spin-coupling constants.

(3) All COSY variants may be combined with different schemes of water suppression.

(4) The phase-sensitive COSY variants can be recorded in high resolution in both dimensions which enables the extraction of digital correct spin-coupling values in the direct dimension.

Fig. 1.3-1 J. Jeener *1931

Almost in despair, I started investigating this latter problem with the help of Gerit Alewaelers, initially on the simple case of the standard AB spectrum in liquids. This soon led to the general proposal of 2D FT NMR spectroscopy in the simple case of homonuclear COSY without phase cycling. We tried to observe the effect experimentally on ethylbenzene, spending weekends working with the rather primitive FT spectrometer available in organic chemistry at our university. Due to the bad phase stability of this spectrometer and to our total lack of practice of high-resolution NMR, Gerit Alewaeters could only observe some of the strongest cross peaks of the 2D spectrum with a signal-to-noise ratio high enough to confirm that our quantum mechanical predictions were correct (not really a surprise.....), but too low to make the new technique look very usable. Formal publication was deferred until cleaner experimental confirmation would be available, but I kept spreading the idea by personal contacts, lectures (probably for the first time at the AMPERE Summer School in Basko Polje in 1971) and by circulating 'unpublished' notes written in November 1971. Soon, Richard Ernst let me know that his co-worker Baumann had brought the 2D FT idea back from Basko Polje to Zürich, and that the Zürich group intended to work on it. As it turned out, one of our recurrent delights in Brussels for a number of years has been receiving news from Zürich about the progress of 2D NMR, both experimental and theoretical. It was also a pleasure to learn about the new 2D FT ideas developing in many other groups.

Jean Jeener, *1931, "Reminiscences about the early days of 2D NMR" *Enyclopedia of NMR*, **1996**, *1*, 409–410.

3. Pulse Scheme and Phase Cycle

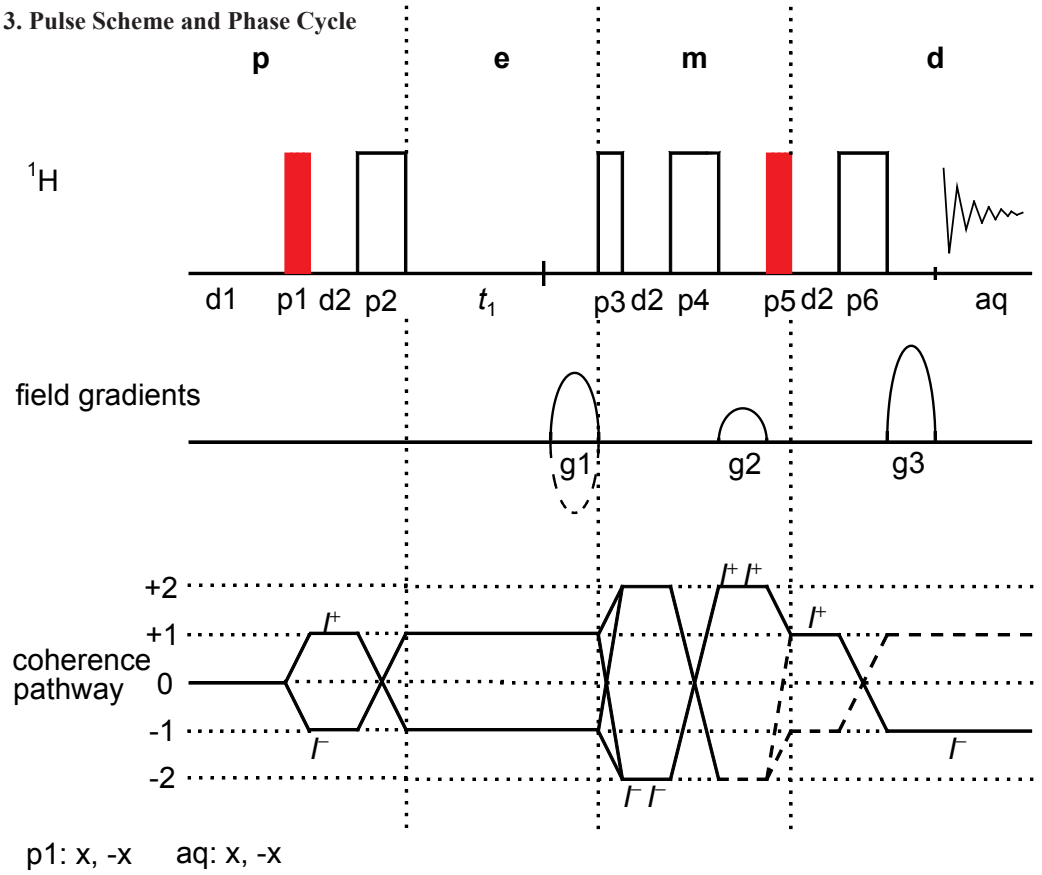

Scheme 1.3-1

Common values:

p1, p3, p5: 90° ^{1}H transmitter pulse
p2, p4, p6: 180° ^{1}H transmitter pulse
d1: relaxation delay
d2: effective length of gradient
t1: evolution increment
g1, g3: gradients for Echo/Antiecho selection
g2: gradient for double quantum selection

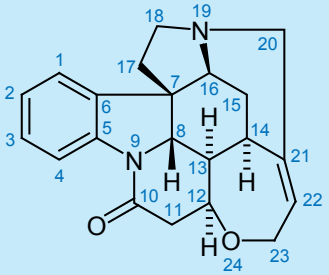

Scheme 1.3-2

4. Acquisition

Special values used for the spectrum shown:

Sample: 3% strychnine in $CDCl_3$.
Time requirement: 20 min
Spectrometer: Bruker DRX-600 with 5-mm-TBI probe

td2:	2K data points in F_2
td1:	256 data points in F_1
sw2:	10 ppm
sw1:	10 ppm
aq1:	0.023 s
aq2:	0.19 s
o1:	middle of ^{1}H NMR spectrum
d1:	2 s
d2:	equal to effective duration of gradient used, here 1.05 ms
g1, g2, g3:	sinusoidal-shaped field gradients, 1 ms duration gradient ratio 30:10:50 with 0.56 T/m = 100%
rg:	One must be very careful in setting the receiver gain for this experiment. The gradient filter allows only the

desired coherences to pass into the receiver; however, the double-quantum coherences develop only at higher t_1 increments because of modulation with sin (πJt_1), cf. Equ. 2 see Question C. The receiver gain must therefore be set using a high t_1 increment to avoid overloading.

ds: 2
ns: 2

5. Processing

Apply zero-filling in F_1 to 1K words in order to have a symmetrical matrix of 1024×1024 data points. Use an exponential window with lb = 3 Hz in the F_2 dimension and a squared π/2 shifted sinusoidal window in the indirect dimension. Apply complex Fourier transformation in both dimensions. Phase correction in both dimensions can be performed after the 2D transformation in order to get clean up/down patterns of the cross-peaks. Zero order phase correction of 90° is a good starting point for the F_1 dimension.

6. Result

The overview spectrum displays all relevant connectivities for strychnine. In the aliphatic expansion clearly the AX pattern can be observed, even though more complicated multipletts are coupled to each other. In the aromatic expansion this is also demonstrated.

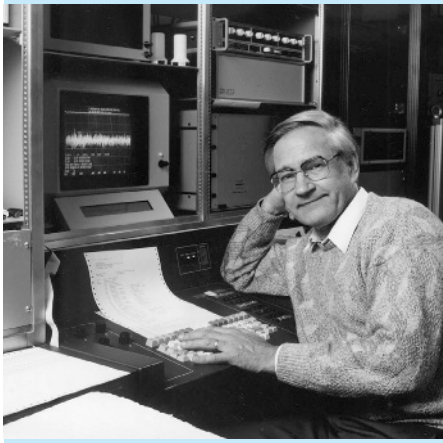

Fig. 1.3-2 R. R. Ernst *1933

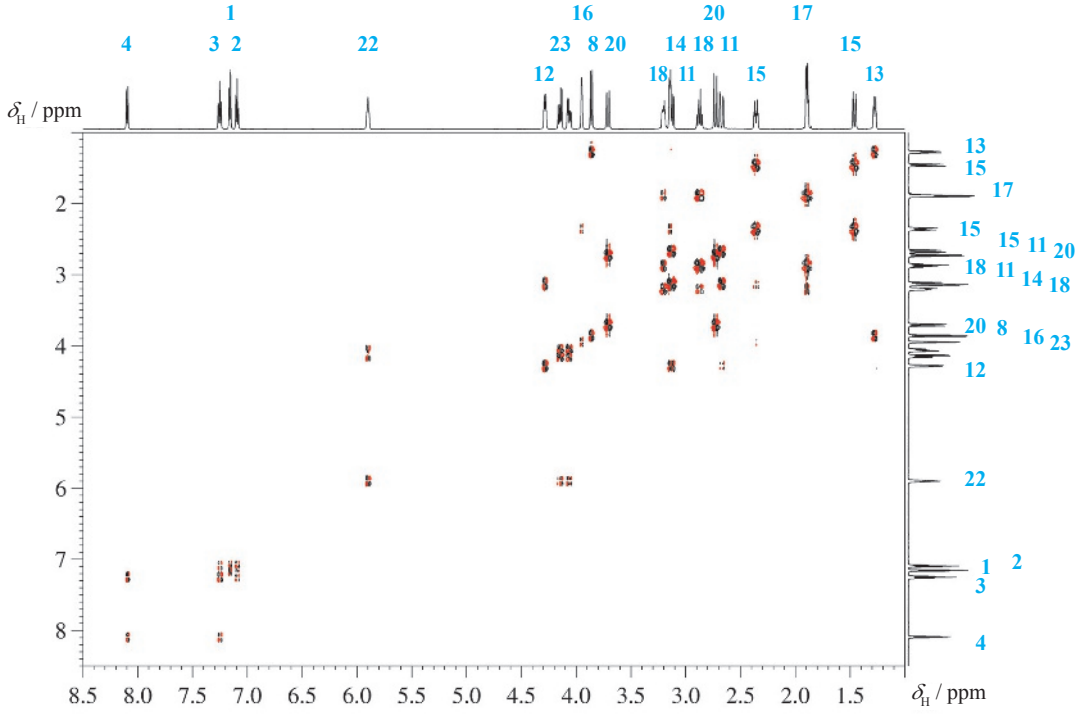

Fig. 1.3-3 COSY spectrum of strychnine

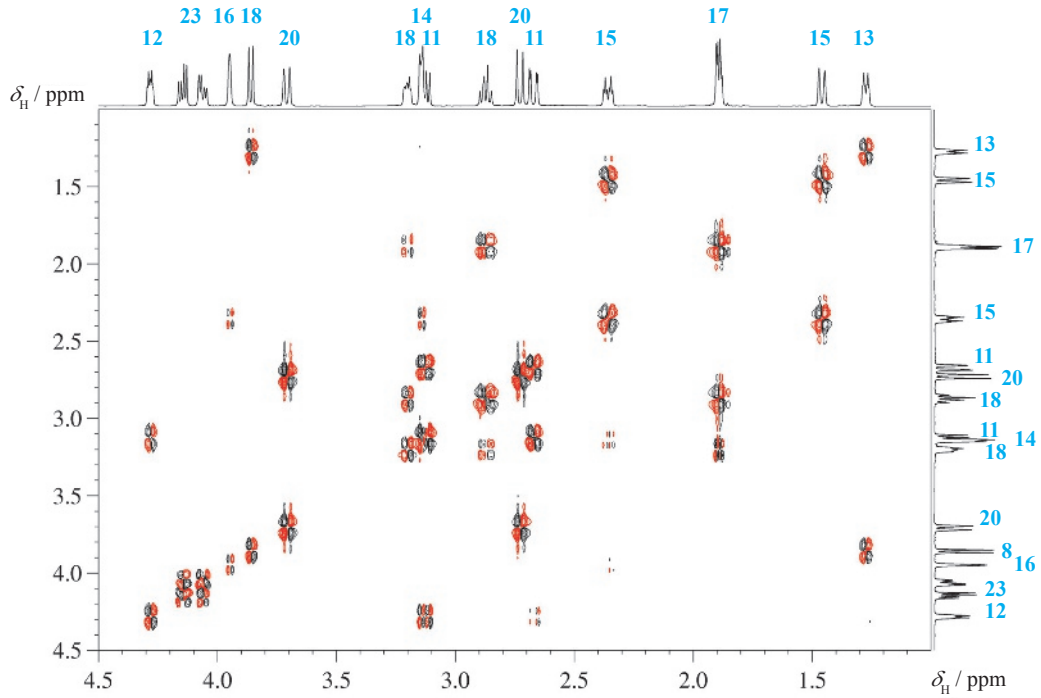

Fig.1.3-4 Expansion of the COSY spectrum in the aliphatic region

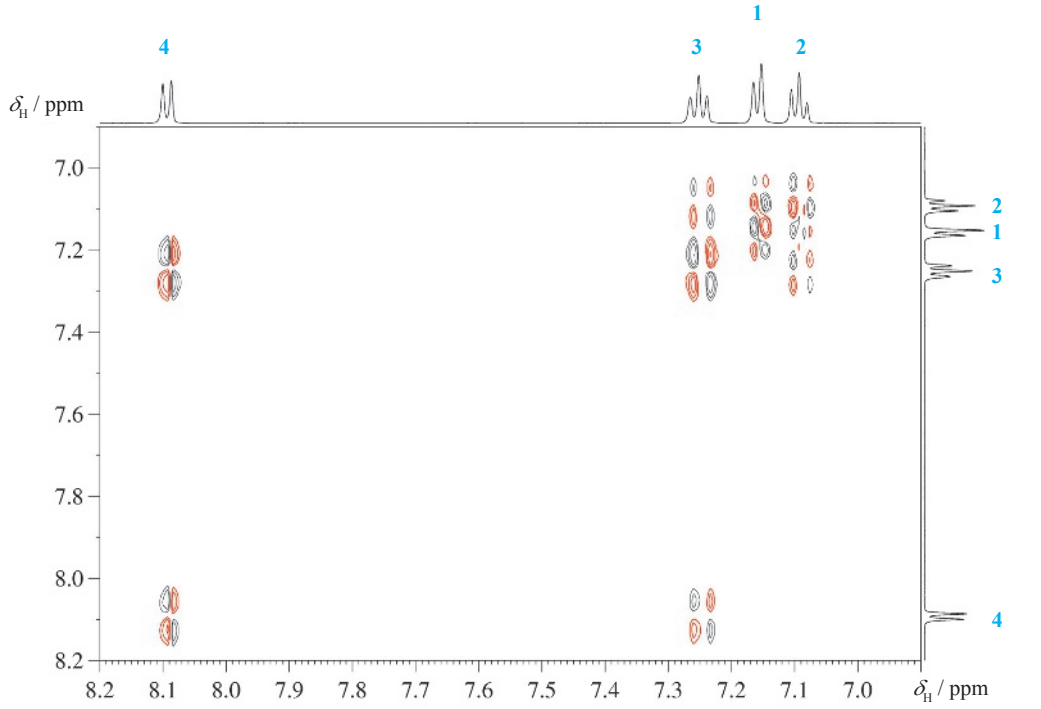

Fig. 1.3-5 Expansion of the COSY spectrum in the aromatic region

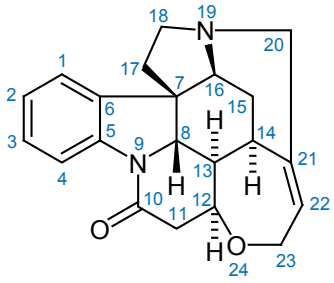

Scheme 1.3-3 Strychnine

The participation of Thomas W. Bauman at the AMPERE summer School in Basko Polje, Yugoslavia, in September 1971 was an extremely fortunate event. Being a meticulous scientist, he brought home a careful script of the lectures, among them one by Jean Jeener that attracted my attention immediately: a simple two-pulse experiment that produced revealing 2D spectra by 2D Fourier transformation of a 2D set of response signals. This was exactly the technique I had been waiting for. I had been thinking for some time about systematic computer-controlled double resonance experiments, but appreciated the complexity of the resulting 2D spectra should they follow the shape of the famous Anderson-Freeman plots.

R.R. Ernst "The success story of fourier transformation in NMR" *Enyclopedia of NMR*, **1996**, *1*, 297.

7. Comments

The two pulses given in red color are the essential COSY pulses used in the original pulse sequence. The additional pulses are used for the double-quantum filter (p3) and for phase correction due to the finite length of the gradient pulses (p2, p4, p6)

In the *preparation period* **p** of the pulse sequence we find the relaxation delay d1 and the first r.f. pulse p1 which transforms *z*-magnetization into transverse magnetization. The delay d2 and the 180° pulse p2 only serve to alleviate the finite length of the gradient pulse g1, which would otherwise cause a problem in phasing the 2D spectrum. Then the chemical shift develops in the *evolution period* **e** during t_1, which is written here only for proton 1, giving Equation (1). In addition, spin–spin coupling develops; thus each of the two terms with a modulation by the chemical shift will create two more terms including the spin–spin coupling.

$$I_{1_z} + I_{2_z} \xrightarrow{I_x} -I_{1_y} - I_{2_y} \xrightarrow{\Omega_1 t_1 I_{1_z}} -I_{1_y}\cos\Omega_1 t_1 + I_{1_x}\sin\Omega_1 t_1 \qquad (1)$$

$$\xrightarrow{\pi J t_1 2I_{1_z}I_{2_z}} -I_{1_y}\cos\Omega_1 t_1\cos\pi J t_1 + 2I_{1_x}I_{2_z}\cos\Omega_1 t_1\sin\pi J t_1 + I_{1_x}\sin\Omega_1 t_1\cos\pi J t_1 + 2I_{1_y}I_{2_z}\sin\Omega_1 t_1\sin\pi J t_1 \qquad (2)$$

In the *mixing period* **m** of the pulse sequence the r.f. pulse p3 creates double-quantum magnetization $-2I_{1_x}I_{2_y}$, as in Equation (3). Again the delay d2 and the 180° pulse p4 are only for phase correction and correct for the finite length of the gradient pulse g2, which encodes the double-quantum magnetization.

$$2I_{1_x}I_{2_z}\cos\Omega_1 t_1\sin\pi J t_1 \xrightarrow{I_x} -2I_{1_x}I_{2_y}\cos\Omega_1 t_1\sin\pi J t_1 \qquad (3)$$

The 90° pulse p5 creates antiphase magnetization from the double-quantum term as given in eq. (4)

(4)

$$-2I_{1_x}I_{2_y}\cos\Omega_1 t_1 \sin\pi J t_1 \xrightarrow{I_x} -2I_{1_x}I_{2_z}\cos\Omega_1 t_1 \sin\pi J t_1$$

In the *detection period* **d** chemical shift and spin–spin coupling develop once again during the acquisition time t_2, giving Equation (5).

(5)

$$\xrightarrow{\Omega_2 t_2 I_{1_z}} \xrightarrow{\pi J t_2 2I_{1_z}I_{2_z}} I_{2_y}\cos\Omega_1 t_1 \sin\pi J t_1 \sin\Omega_2 t_2 \sin\pi J t_2$$

The last expression describes a cross-peak in the COSY matrix.

With the pulse sequence and the echo-antiecho scheme of the gradients used, the sign of the frequencies in F_1 is determined by keeping the sine and cosine terms separate, and thus allows phase-sensitive processing.

As can be seen from the coherence pathway diagram above, the first gradient g1 acts during a period when single-quantum magnetization I^+ is present (coherence level +1), whereas the second acts during a period when double-quantum coherence I^+I^+ is present. The final gradient pulse acts on I^-. Therefore the gradient ratios 30:10:50 and -30:10:50 will be successful to obtain the desired signals. All other coherences are further dephased and are not observable.

8. Questions

A. Why does the standard COSY not reveal strong cross peaks for long-range spin couplings and what is the trick, whereby the long-range COSY is functioning?

B. In which dimension one would extract spin coupling values from a high-resolution COSY and why?

C. Why are double quantum coherences only developing at higher t_1 increments?

D. In the aromatic expansion of the strychnine spectrum one observes only an AX pattern from the triplet. Why?

E. Only one of the protons H-15 displays a cross peak to H-16. Why?

9. Own Observations

[1] J. Jeener, *Ampère International Summer School*, Basko Polje, **1971** (proposal).

[2] W. P. Aue, E. Bartholdi, R. R. Ernst "Two-dimensional spectroscopy. Application to nuclear magnetic resonance" *J. Chem. Phys.* **1975**, *64*, 2229–2246.

[3] T. D. W. Claridge, "High-Resolution NMR techniques in organic chemistry", Pergamon, Oxford, **1999**, 155–159.

[4] J. Keeler, "Understanding NMR spectroscopy", Wiley, Chichester, 2nd Ed. 2010.

Experiment 1.4

NOESY

1. Purpose

The NOESY (**N**uclear **O**verhauser **E**nhancement **S**pectroscop**Y**) experiment is the two-dimensional equivalent of the NOE difference experiment (see chapter 3.6) and yields correlation signals that are caused by dipolar cross-relaxation between nuclei in a close spatial relationship.

The intensities of the cross-peaks under certain conditions are proportional to the sixth power of the proton–proton distances. Quantitatively, the results differ from 1D NOE difference spectroscopy, since the latter is a steady-state experiment obtained from a saturation of the energy levels, whereas NOESY is a transient experiment obtained after population inversion of the energy levels. In a qualitative way, the NOESY technique gives answers to many stereochemical problems such as *exo/endo*, *E/Z* and similar assignment questions. In NMR studies of peptides and proteins NOESY is the essential method for determining peptide conformations or tertiary structure of proteins. We show here a phase-sensitive version with two spoiling gradients during the mixing time.

Fig. 1.4-1 A. W. Overhauser (1925-2011)

2. Variants

The gradient pulses during the mixing time destroy most of the COSY artefacts present in NOESY, however, not the zero-quantum coherences. Further improvements of a gradient-supported NOESY technique have been described recently [4]. The NOESY technique has been combined with different schemes of water suppression, if biological samples have to be measured. Also, in protein NMR a 3D version with ^{15}N editing is the standard technique. Selective 1D NOESY sequences are known if only the answer of a particular spin is needed. An echo-antiecho method as shown in chapter 1.3 for COSY is not advisable because of diffusion effects during the mixing time (encoding gradients before and after the mixing time).

A considerable drawback of the NOESY technique is the dependence of the NOE effect on molar mass and viscosity, which can change its sign and may cause it to disappear for certain conditions. The ROESY technique as described in Experiment 2.2 may be more effective in this case.

In both, chemical exchange of nuclei may yield cross peaks, too.

Fig. 1.4-2 R. R. Ernst *1933

3. Pulse Scheme and Phase Cycle

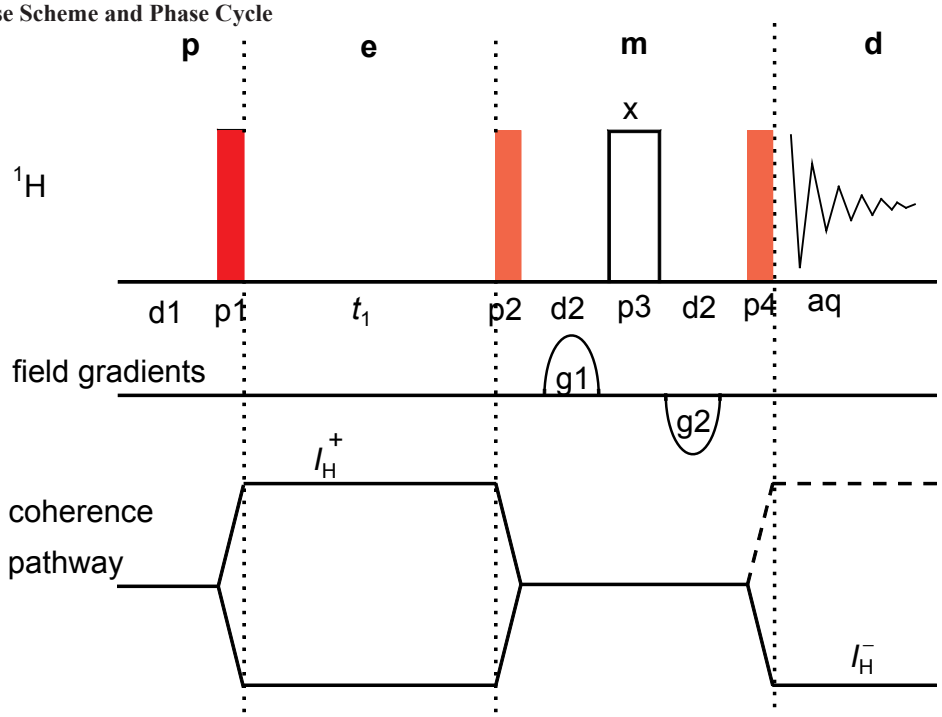

p1: x, -x p2: $(x)_8$, $(-x)_8$ p4: x, x, -x, -x, -y, -y, y, y

aq: x, -x, -x, x, y, -y, -y, y, -x, x, x, -x, -y, y, y, -y

phase cycle for p1 incremented according to States-TPPI

Scheme 1.4-1

Common values:

p1, p2, p4: 90° ^{1}H transmitter pulse
p3: 180° ^{1}H transmitter pulse
d1: relaxation delay
d2: mixing time 2, in the order of ^{1}H relaxation time
t1: evolution increment
g1, g2: gradients for artifact suppression

4. Acquisition

Special values used for the spectrum shown:

Sample: 3% strychnine in $CDCl_3$.
Time requirement: 5 h
Spectrometer: Bruker DRX-600 with 5-mm-TBI-probe

td2:	2K data points in F_2
td1:	256 data points in F_1
sw2:	10 ppm
sw1:	10 ppm
aq2:	0.17 s
aq1:	0.021 s
o1:	middle of ^{1}H NMR spectrum
d1:	2 s
d2:	1 s
ds:	4
ns:	8
g1, g2:	40 : (-40) with 0.6 T/m = 100 %

5. Processing

Apply zero-filling in F_1 to 1K real data points to obtain a symmetrical matrix of 1K×1K real data points. Use an exponential window in F_2 with lb = 5 Hz and a π/2-shifted squared sine bell in F_1.

Apply complex Fourier transformation corresponding to the States-TPPI mode of data acquisition in F_1. Adjust the phase of the diagonal signals so that they are negative. The NOESY correlation signals will then be positive if the compound has a molar mass below 1000 (positive NOE effect). Correlation signals caused by chemical exchange will have the same phase as the diagonal signals.

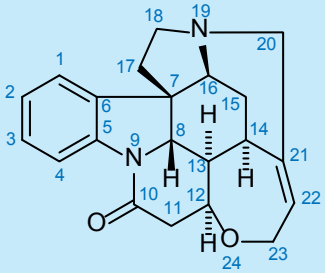

Scheme 1.4-2

6. Result

The figures show the result obtained on a DRX-600 spectrometer. Note that the phase of the diagonal signals is opposite to that of the cross-peaks as can be seen from the dotted contours. There is a wealth of information to be taken from the spectrum, which can best be studied using a molecular model or an electronic 3D file. Notice, for instance, that only one of the H-20 protons has an NOE contact with one of the H-15 protons, from which a relative assignment of the protons in these methylene groups can be derived.

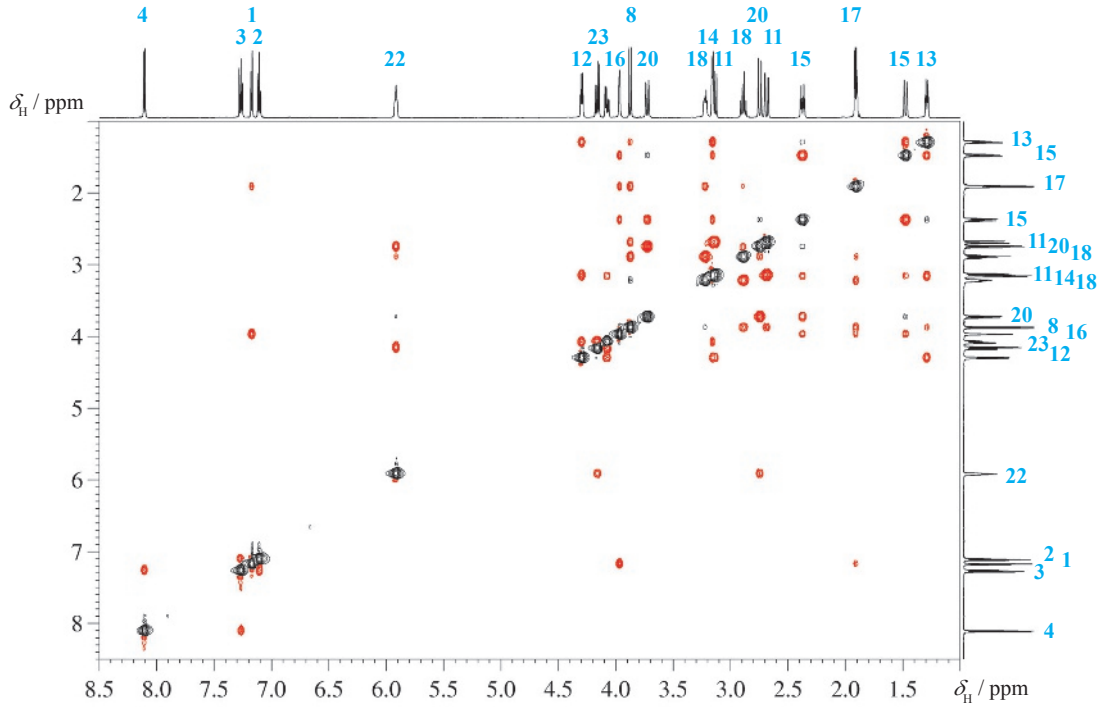

Fig. 1.4-3 NOESY spectrum of strychnine

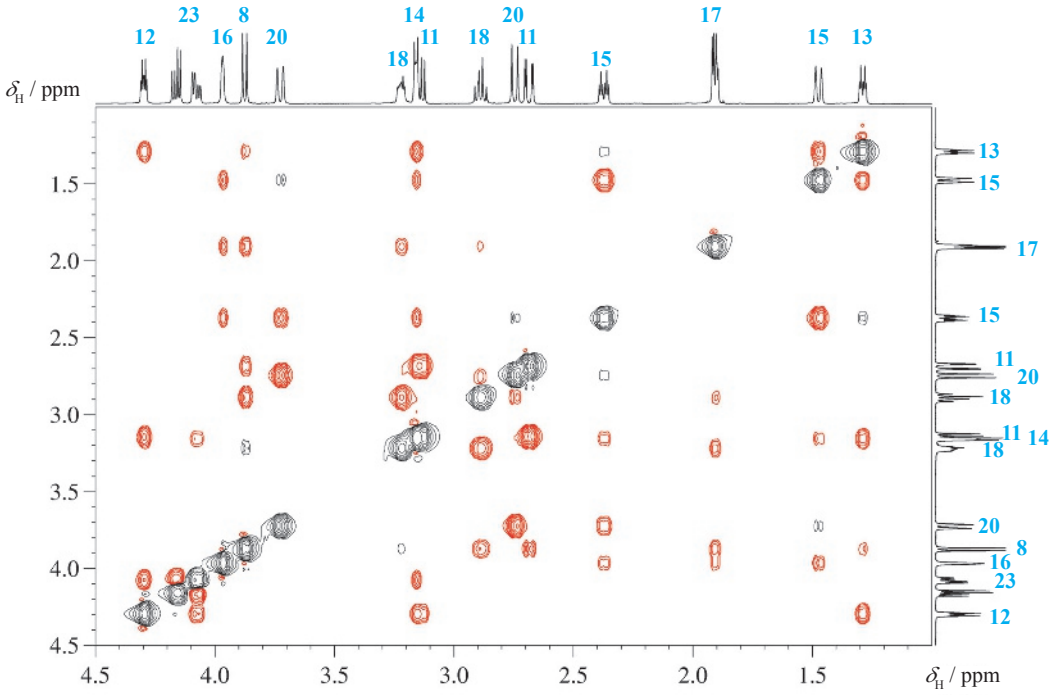

Fig. 1.4-4 Expansion of the spectrum in the aliphatic region

Albert Overhauser, a young theoretician from the University of Illinois, had made the following prediction: in a metal, where the conduction electrons are known to be responsible for the nuclear relaxation, the saturation of the ESR resonance of these electrons should lead to an enormous increase in the nuclear polarization. [...] Secondly, that Overhauser's audience at the meeting of the American Physical Society − where he had (in ten minutes) presented the calculations which had led to his amazing conclusion − was immediately split into two parts, which, however, overlapped: those who did not understand a single word of his demonstration, and those who did not believe a single word of his conclusions. In the first row of the sceptics who did not believe his conclusions shone all the stars of magnetic resonance: Bloch and Purcell, Rabi and Ramsey. Bloembergen was of two minds and so was I. As for the presentation itself, 1 will repeat what Van de

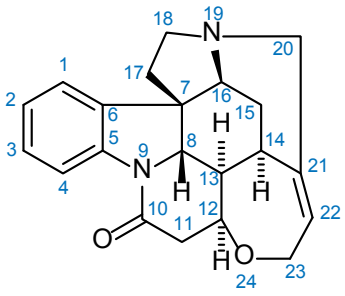

Scheme 1.4-3

7. Comments

The NOESY sequence can be understood from the vector model. We consider two protons with different chemical shifts and without spin–spin coupling.

The *preparation period* **p** starts with the relaxation delay d1. The first pulse p1 of the NOESY sequence shown in red aligns all proton magnetization into the *x,y*-plane which is the end of the time slot **p**.

In the *evolution period* **e**, chemical shift and spin−spin coupling evolve during t_1. In the *mixing period* **m** the second red pulse p2 aligns the *y* components of the two vectors, which are by now labelled with their individual chemical shifts into the negative *z*-direction. This situation is called a chemical shift-encoded *z*-magnetization. In the second scan of the phase cycle pulse p2 aligns the *y* components to the positive *z* direction to get a FID without NOE effect. Both scans are subtracted by receiver phase to yield the difference spectrum. During the mixing time (2×d2) both protons are allowed to relax and show cross relaxation.

This pathway is shown in the coherence diagram. In addition, however, the pulse p2 can generate zero-, double-quantum- and antiphase coherences, since H,H spin coupling is also evolved during t_1. The positive and negative gradient pulses in the mixing time, which embrace the 180° pulse p3, dephase all these components except the zero-quantum coherences. Furthermore, they dephase axial signals of those protons that have relaxed during t_1 and are excited again by p2. The final pulse p4 reads the situation at the end of the mixing time and realigns the vectors into the *x,y* plane, where the FID is recorded.

Graaff had told me of de Broglie's defensc of his thesis in Paris in 1924. „Never had so much gone over the heads of so many".

The real question was of course: „Was Overhauser right?" He was: the proof of the pudding was given the same year by Charles Slichter, a physicist from Illinois, and his student, Carver. They saturated the resonance of conduction electrons in metallic lithium and saw the enhancement of the nuclear polarization predicted by Overhauser.

A. Abragam, (1914-2011) "Time reversal, an autobiography", Oxford University Press **1989**

[1] J. Jeener, B. H. Meier, P. Bachmann, R. R. Ernst "Investigation of exchange processes by two-dimensional NMR spectroscopy" *J. Chem. Phys*. **1979**, *71*, 4546–4553.

[2] D. J. States, R. A. Haberkorn, D. J. Ruben "A two-dimensional nuclear Overhauser experiment with pure absorption phase in four quadrants" *J. Magn. Reson*. **1982**, *48*, 286–292.

[3] G. Bodenhausen, H. Kogler, R. R. Ernst "Selection of coherence-transfer pathways in NMR pulse experiments" *J. Magn. Reson.* **1984**, *58*, 370–388.

[4] R. Wagner, S. Berger "Gradient-selected NOESY—A fourfold reduction of the measurement time for the NOESY experiment" *J. Magn. Reson*. Ser. A **1996**, *123*, 119–121.

[5] T. Parella, F. Sánchez-Ferrando, A. Virgili "Quick recording of pure absorption 2D TOCSY, ROESY, and NOESY spectra using pulsed field gradients" *J. Magn. Reson*. **1997**, *125*, 145–148.

[6] M. J. Thrippleton, J. Keeler "Elimination of zero quantum interference in two-dimensional NMR spectra" *Angew. Chem. Int. Ed*. **2003**, *42*, 3938–3941.

[7] D. Neuhaus, M.P. Williamson, "The nuclear Overhauser effect in structural and conformational analysis", 2nd Ed., Wiley-VCH, Weinheim, **2000**.

8. Questions

A. Explain why the mixing time is best approached by the spin-lattice relaxation time of the spins involved.

B. What is meant by a NOESY build-up curve and how is it obtained?

C. What is the reason that build-up curves have a maximum and decay to zero at long mixing times?

D. If the ROESY technique does not have the sign problem that NOESY has, why does one not use only ROESY in all situations?

E. Which molecular entities are suitable for a distance reference?

9. Own Observations

Experiment 1.5

HSQC

1. Purpose

C,H correlation, as well as other X,H correlations, is now mainly achieved by the HSQC (**H**eteronuclear **S**ingle **Q**uantum **C**oherence) method, because in this sequence the signals are not broadened by homonuclear H,H coupling in F_1. The HSQC scheme is included as a building block in many 3D sequences, especially for structural biology, but has become established as the standard scheme of C,H correlation in organic chemistry. In the experiment shown here (using strychnine as example) we demonstrate a combination of several features which persuade us that it is today the method of choice.

Fig. 1.5-1 G. Bodenhausen (*1951)

The enhancement in sensitivity possible with this scheme dwarfs the enhancement obtainable with the nuclear Overhauser effect (when observing the low-γ nucleus directly), and therefore it has been referred to as the *Overbodenhausen* experiment.

Ad Bax et al., *J. Magn.Reson*. **1990**, *86*, 304-318.

2. Variants

Since the introduction of this experiment [1], there has been a permanent development. Today, mostly a gradient-selected variant is used, with the gradients operating in the echo-antiecho method for sensitivity reasons.

Additional sensitivity improvement by a factor of $\sqrt{2}$ is achieved by a double back INEPT transfer; however, this occurs only for CH groups [2-5]. In reference [6], applications for long-range spin couplings are discussed. In most cases it is desirable to obtain an editing of 2D H,X correlation spectra. This can yield a multiplicity determination in case of overlapping ^{13}C signals, or reveal CH moieties in the presence of many CH_2 groups or NH_2 groups in the middle of many NH groups in proteins. This kind of multiplicity determination can be achieved by including an editing period.[7-10]

In contrast to HMQC, the HSQC experiment employs 180° pulses, which causes problems if the 180° pulses become too long (e.g., in a triple-tuned probe) but have to cover a very wide spectral range. This leads to severe phasing problems for instruments with a magnetic field above that corresponding to 500 MHz ^1H frequency. The remedy for this problem is to apply frequency-swept adiabatic 180° ^{13}C pulses (see chapter 8.4), which can cover the large spectral width of ^{13}C [11, 12].

3. Pulse Scheme and Phase Cycle

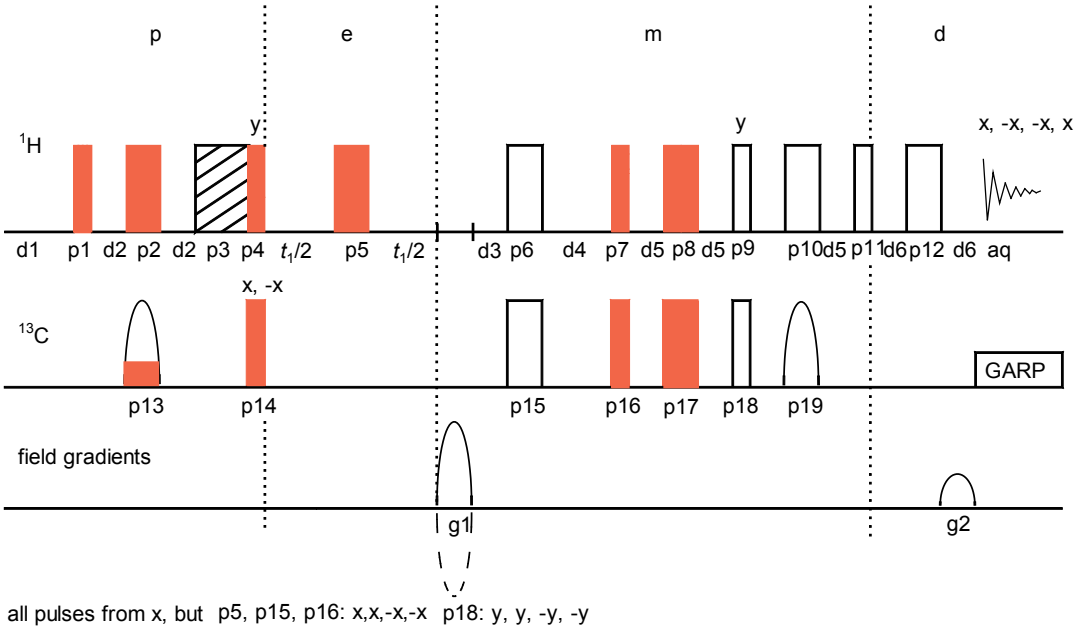

Scheme 1.5-1

Common values:

p1, p4, p7, p9, p11: 90° ^{1}H transmitter pulse
p2, p5, p6, p8, p10, p12: 180° ^{1}H transmitter pulse
p3: trim pulse
p14, p16, p18: 90° ^{13}C transmitter pulse
p15, p17: 180° ^{13}C transmitter pulse
p13, p19 ^{13}C-CHIRP pulse for inversion
d1: relaxation delay
d2, d5: polarization delay during INEPT or back INEPT transfer
d3, d4: editing delay for multiplicity recognition
t_1: evolution increment
g1,g2: gradients for echo/antiecho selection

4. Acquisition

Special values used for the spectrum shown:

Sample: 3% strychnine in $CDCl_3$.
Time requirement: 80 min
Spectrometer: Bruker DRX-600 with 5-mm TBI probe

td2: 2K data points in F_2
td1: 256 data points in F_1
sw2: 9 ppm
sw1: 160 ppm
aq2: 0.13 s
aq1: 0.005 s
offset of ^{1}H frequency: middle of ^{1}H NMR spectrum [4.5 ppm]
offset of ^{13}C frequency: middle of ^{13}C NMR spectrum [80 ppm]
p3: ^{1}H trim pulse [1 ms, 5 dB]
p13, p19: adiabatic chirped 180° ^{13}C pulse [crp 60, 0.5, 20.1; 500 µs, 5.5 dB]
^{13}C decoupler attenuation and 90° pulse for GARP [14.3 dB, 70 µs]
d1: 2 s
d2: $1/[4J(C,H)] = 1.72$ ms, calculated from $^1J(C,H) \approx 145$ Hz
d3: $1/[2J(C,H)]$ minus effective gradient length g1 (=1.05 ms) = 2.39ms
d4: $1/[2J(C,H)] = 3.44$ ms calculated from $^1J(C,H) \approx 145$ Hz
d5: $1/[8J(C,H)] = 0.862$ ms calculated from $^1J(C,H) \approx 145$ Hz
d6: effective length of pulsed field gradients, here 1.05 ms
g1, g2: 80 : 20.1; g1 switched to negative according to echo-antiecho scheme
ds: 8
ns: 8

5. Processing

Apply zero-filling in F_1 to 1K words in order to have a symmetrical matrix of 1024×1024 data points. Use an exponential window with lb = 3 Hz in the F_2 dimension and a squared π/2 shifted sinusoidal window in the indirect dimension. Apply real Fourier transformation in both dimensions. Phase correction in both dimensions can be performed, after the 2D transformation, to positive and negative signals for the CH or CH_3 and the CH_2 groups.

6. Result

The figures show the spectrum obtained on an DRX-600 spectrometer with a multinuclear inverse probe equipped with *z*-gradients. The overview spectrum displays all relevant connectivities for strychnine. Since the compound is chiral, all CH_2 groups are diastereotopic, which can be nicely observed for the red signals. Due to the adiabatic 180° pulses on ^{13}C, there are no phase problems.

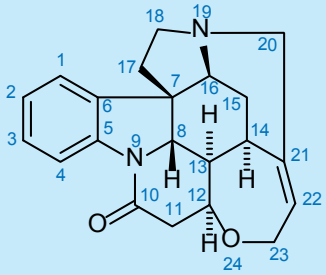

Scheme 1.5-2

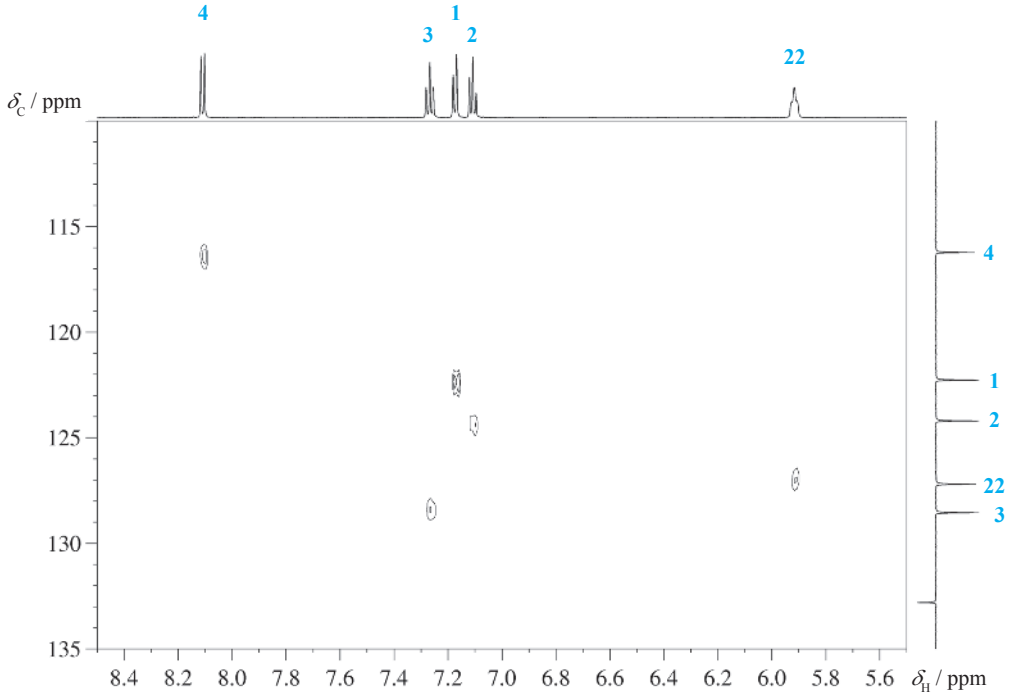

Fig. 1.5-2 Expansion of the HSQC spectrum in the aromatic region

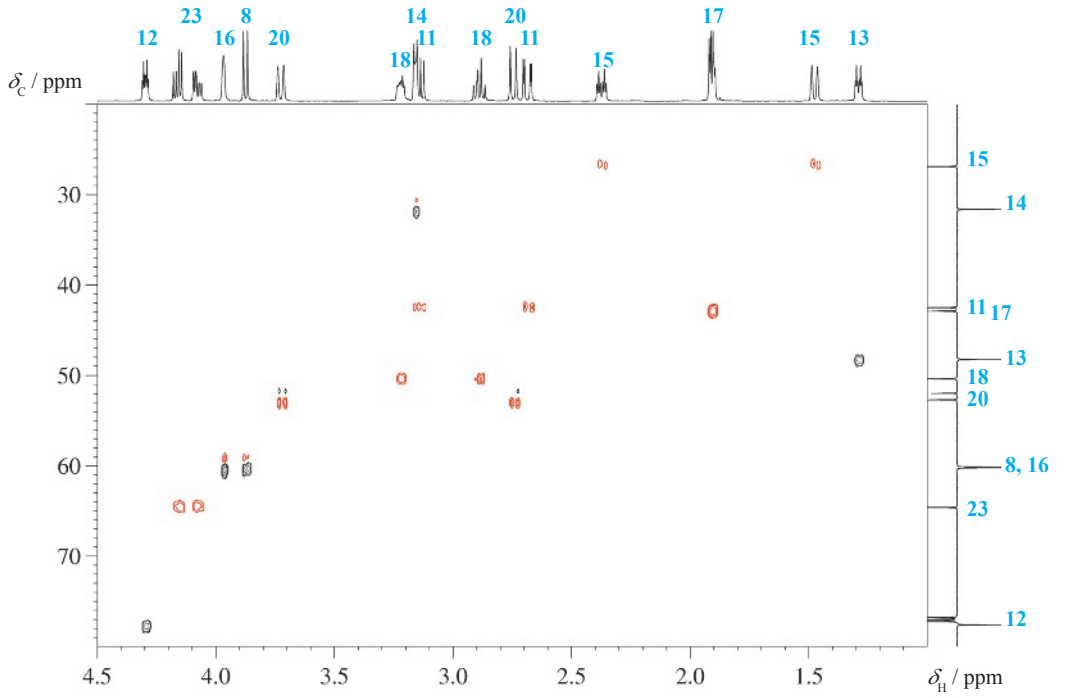

Fig. 1.5-3 Expansion of the HSQC spectrum in the aliphatic region

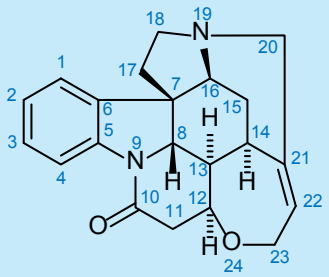

Scheme 1.5-3

7. Comments

The pulses given in red color are the essential HSQC pulses used in the original pulse sequence. p3 acts as a trim pulse during the INEPT transfer, p6 and p15 are refocusing pulses during the editing period, and all others are for the double INEPT back transfer. The 180° pulses p13 and p19 are shaped adiabatic pulse to alleviate phase problems and cover the large ^{13}C chemical shift range.

In the preparation period **p** the sequence starts with an INEPT transfer from proton to ^{13}C. This INEPT transfer results in antiphase magnetization of ^{13}C with respect to proton; thus $-2I_{H_z}I_{C_y}$ single-quantum coherence is present at the end of this section. The trim pulse p3 removes unwanted magnetization.

In the evolution period **e** one t_1 section follows with a 180° pulse on the protons in the middle of t_1. During t_1 the term $-2I_{H_z}I_{C_y}$ develops ^{13}C chemical shift as described by Equation (1). The 180° proton pulse p5 eliminates the J(C,H) couplings in F_1 and for simplicity is not shown in the equations.

(1)

$$-2I_{H_z}I_{C_y} \xrightarrow{\Omega_C t_1 I_{C_z}} -2I_{H_z}I_{C_y}\cos\Omega_C t_1 + 2I_{H_z}I_{C_x}\sin\Omega_C t_1$$

After the chemical shift evolution an editing period in the mixing period **m** serves for different signs of CH and CH_3 or CH_2 signals. The editing period starts with gradient g1, delay d3, consists of the two pulses p6

and p15, and ends with the delay d4. The length of (g1 + d3) is equal to d4. If, for instance, the delays are set to 1/2*J,* the total length of the editing period is 1/*J* as in the APT method (see chapter 1.2), and CH_2 spin vectors will point in the opposite direction compared to those of CH and CH_3 moieties.

After the editing period **e** a double back INEPT transfer occurs from ^{13}C to proton.

The first INEPT back transfer converts the term of equation (1) by the pulses p16 and p7 into $(2I_{H_y}I_{C_z}\cos\Omega_C t_1 - 2I_{H_y}I_{C_x}\sin\Omega_C t)$, where the second part is a double-quantum magnetization. In the first spin echo period with the 180° pulses p17 and p8 these terms are therefore converted into $(I_{H_x}\cos\Omega_C t_1 - 2I_{H_y}I_{C_x}\sin\Omega_C t)$. The second INEPT back transfer starts with the pulses p18 and p9 and these store I_{H_x} as *z*-magnetization and convert the double-quantum term into antiphase magnetization: $(I_{H_z}\cos\Omega_C t_1 - 2I_{H_y}I_{C_z}\sin\Omega_C t)$. The latter develops in the second spin-echo period, interrupted by the pulses p19 and p10 and by the final 90° pulse p11 into $(-I_{H_y}\cos\Omega_C t_1 + I_{H_x}I_{C_z}\sin\Omega_C t)$.

Thus both the sin and the cos chemical shift terms contribute to the intensity of the signal, and this is called "sensitivity enhancement (SI)" or "preservation of equivalent pathways (PEP)" or "coherence selective transfer (COS)" by different authors.

The detection period **d** consists of the d6-p12-gradient g2 sandwich and the acqusition with GARP decoupling.

Fig. 1-5.4 "Die zweite Dimension", Harald Jancke, Berlin 1985

[1] G. Bodenhausen, D. J. Ruben "Natural abundance nitrogen ^{15}NMR by enhanced heteronuclear Spectroscopy" *Chem. Phys. Lett.* **1980**, *69*, 185–189.

[2] L. E. Kay, P. Keifer, T. Saarinen"Pure absorption gradient enhanced heteronuclear single quantum correlation spectroscopy with improved sensitivity" *J. Am. Chem. Soc*. **1992**, *114*, 10663–10665.

[3] A. G. Palmer III, J. Cavanagh, P. E. Wright, M. Rance "Sensitivity improvement in proton-detected two-dimensional heteronuclear correlation NMR spectroscopy" *J. Magn. Reson*. **1991**, *93*, 151–170.

[4] G. Kontaxis, J. Stonehouse, E. D. Laue, J. Keeler "The sensitivity of experiments which use gradient pulses for coherence pathway selection" *J. Magn. Reson*. Ser. A **1994**, *111*,70–76.

[5] J. Schleucher, M. Schwendinger, M. Sattler, P. Schmidt, O. Schedletzky, S. J. Glaser, O. W. Sørensen, C. Griesinger "A general enhancement scheme in heteronuclear multidimensional NMR employing pulsed-field gradients" *J. Biomol. NMR* **1994**, *4*, 301–306.

[6] R. Marek, L. Králik, V. Sklenár "Gradient-enhanced HSQC experiments for phase-sensitive detection of multiple bond interactions" *Tetrahedron Lett*. **1997**, *38*, 665–668.

[7] D. G. Davies "Simplification of proton-detected, natural abundance carbon-13 correlation spectra of proteins via multiplet editing" *J. Magn. Reson*. **1990**, *90*, 589–596 "Improved multiplet editing of proton-detected, heteronuclear shift-correlation spectra" *ibid*. **1991**, *91* 665–672.

[8] X. Zhang, C. Wang "^{1}H-detected editable heteronuclear multiple-quantum correlation experiment at natural abundance" *J. Magn. Reson*. **1991**, *91*, 618–623.

[9] W. Willker, D. Leibfritz, R. Kerssebaum, W. Bermel "Gradient selection in inverse heteronuclear correlation spectroscopy" *Magn. Reson. Chem*. **1993**, *31*, 287–292.

[10] T. Parella, J. Belloc, F. Sánchez-Ferrando, A. Virgili "A general building block to introduce carbon multiplicity information into multi-dimensional HSQC-type experiments" *Magn. Reson. Chem*. **1998**, *36*, 715–719.

[11] R. Fu, G. Bodenhausen "Broadband decoupling in NMR with frequency-modulated 'chirp' pulses" *Chem. Phys. Letters* **1995**, *245*, 415–420.

[12] E. Kupce, R. Freeman "Optimized Adiabatic Pulses for Wideband Spin Inversion" *J. Magn. Reson.* Ser. A **1996**, *118*, 299–303.

8. Questions

A. Discuss the difference between the basic HSQC and HMQC sequence. Why is HSQC preferred over HMQC?

B. Why is the PEP mechanism only advantageous for CH groups, but not for CH_2 groups?

9. Own Observations

Experiment 1.6

HMBC

1. Purpose

HMBC [**H**eteronuclear **M**ultiple **B**ond **C**orrelation] is the last experiment within our organic set of essential NMR techniques. It is probably the most important one and typically gives the final answers with respect to a structural problem. The pulse sequence was developed to obtain H,C correlations via ^{2}J(C,H) and ^{3}J(C,H). Sometimes even ^{4}J(C,H) correlations are revealed. An unresolved problem is the incomplete suppression of correlations via ^{1}J(C,H). The experiment is therefore usually performed without broadband ^{13}C decoupling to distinguish long-range correlations from signals originating from ^{1}J(C,H).

Here we describe a recent gradient-selected version [6], which is phase-sensitive using the echo-antiecho mode, but will be with a double low pass filter typically processed in the magnitude mode.

2. Variants

In more than 25 years of development there has been a large variety of proposals concerning how to obtain the long-range CH correlation information most effectively. The main issues are:

(1) The variability of the long-range *J* parameter in organic molecules which ranges from 1 to 20 Hz. Methods which should cope with this include full 3D techniques, where the *J* parameter is evolved in an extra dimension, or semi 3D techniques, where the *J* parameter is incremented at the same time as t_1 like ACCORDION-HMBC [8] and varieties thereof. After extensive experimentation it seems that the recording and co-adding of three different HMBC spectra focused with 2 Hz, 6 Hz and 10 Hz is the most time- and effort - effective solution to this problem.

(2) The variability of the ^{1}J parameter which affects the suppression of ^{1}J break-throughs. Different low-pass filter methods have been proposed and also methods which do not filter at all but separate the two kinds of information (HMSC [9]).

(3) The separation of ^{2}J and ^{3}J correlations, which has been proposed by a sequence called H2BC [10].

(4) The overall sensitivity of the method.

(5) The use of *J*-HMBC for the digital measurement of the long-range CH spin-coupling constants; the combination with *J*-resolved spectroscopy and the high resolution band HMBC (see chapter 3.9) are further current developments.

Fig. 1.6-1: A. Bax, *1956

Although the same HMQC pulse schemes, together with a large number of alternative schemes were proposed independently by the Australian group of Bendall, Pegg, and Doddrell, the application of our experiment to a biological macromolecule and to natural abundance peptides was probably the main reason for the surge in popularity of these HMQC experiments. For me it was my first encounter with a biological application of NMR, and I liked it.

Ad Bax, "NMR of Ethanol and Interferon γ", *Enyclopedia of NMR,* **1996**, *1*, 202–207.

3. Pulse Scheme and Phase Cycle

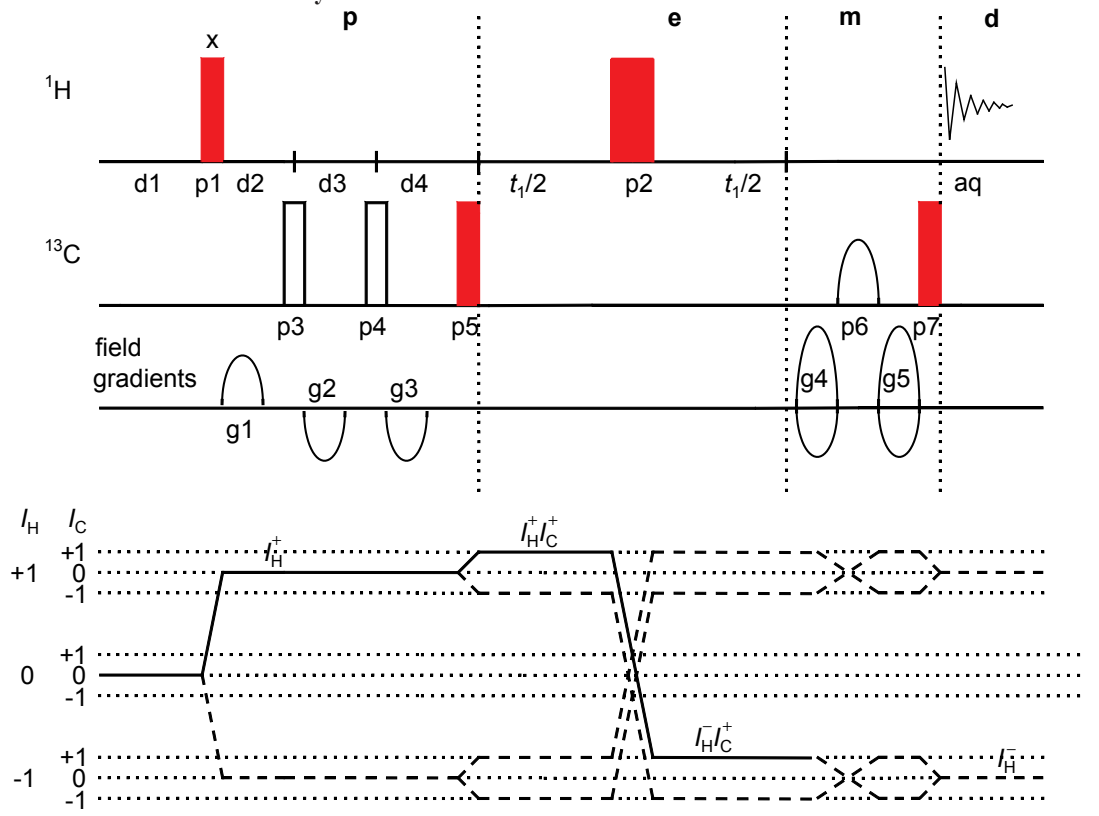

p2: x, x, x, x, -x, -x, -x, -x p3, p4: x, x, -x, -x p5: x, -x p6, p7: $(x)_8$, $(-x)_8$ aq: $(x, -x)_8$, $(-x, x)_8$

Scheme 1.6-1

Common values:

p1: 90° ^{1}H transmitter pulse
p2: 180° ^{1}H transmitter pulse
p3, p4, p5, p7: 90° ^{13}C transmitter pulse
p6: 180° ^{13}C-CHIRP pulse for refocusing
d1: relaxation delay
d2: 1/[2**J*] , minimum ^1J(C,H)
d3: 1/[2**J*] , maximum ^1J(C,H)
d4: 1/[2**J*] , ^nJ(C,H)
t1: evolution increment
g1,g2,g3: gradients for ^1J-low pass filter
g4,g5: switched to positive/negative according to echo/anti-echo scheme

4. Acquisition

Special values used for the spectrum shown:

Sample: 3 % strychnine in $CDCl_3$
Time requirement: 90 min
Spectrometer: Bruker DRX-600 with 5-mm TBI probe

td2: 2K data points in F_2
td1: 512 [2 ×256] data points in F_1
ns: 4
sw2: 9 ppm
sw1: 180 ppm
aq2: 0.19 s
aq1: 0.009 s
offset of ^{1}H frequency: middle of ^{1}H NMR spectrum
offset of ^{13}C frequency: middle of ^{13}C NMR spectrum
p7: 2 ms composite CHIRP , 60 KHz sweep, "Crp60comp.4"
d1: 2.5 s
d2: 4 ms, calculated from ^1J(C,H) ≈ 125 Hz
d3: 2.94 ms, calculated from ^1J(C,H) ≈ 170 Hz

d4: 62.5 ms, calculated from J(C,H) ≈ 8 Hz
g1 to g5: sine-shaped field gradients, 1 ms, 50µs ring-down delay,
g1: 15%, g2: −10 %, g3: −5 %, g4: 80 % and −42 %, g5: −42 % and 80 % (100 % ≈ 0.56 T/m)

5. Processing

Apply zero-filling in F_1 to 1K data points in order to have a matrix of 1K×1K real data points. Before Fourier transformation use an exponential window in F_2 with lb = 3 Hz and π/2-shifted squared sine window in F_1. Phase correction is unnecessary, since the spectrum is processed in magnitude mode in F_1.

6. Result

The figures show extensions of the 2D spectrum obtained on a DRX-600 spectrometer with an inverse multinuclear z-gradient probe. Note the wealth of information obtainable from ^2J and ^3J couplings in this molecule.

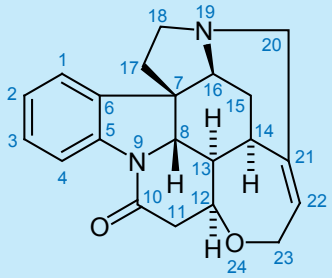

Scheme 1.6-2

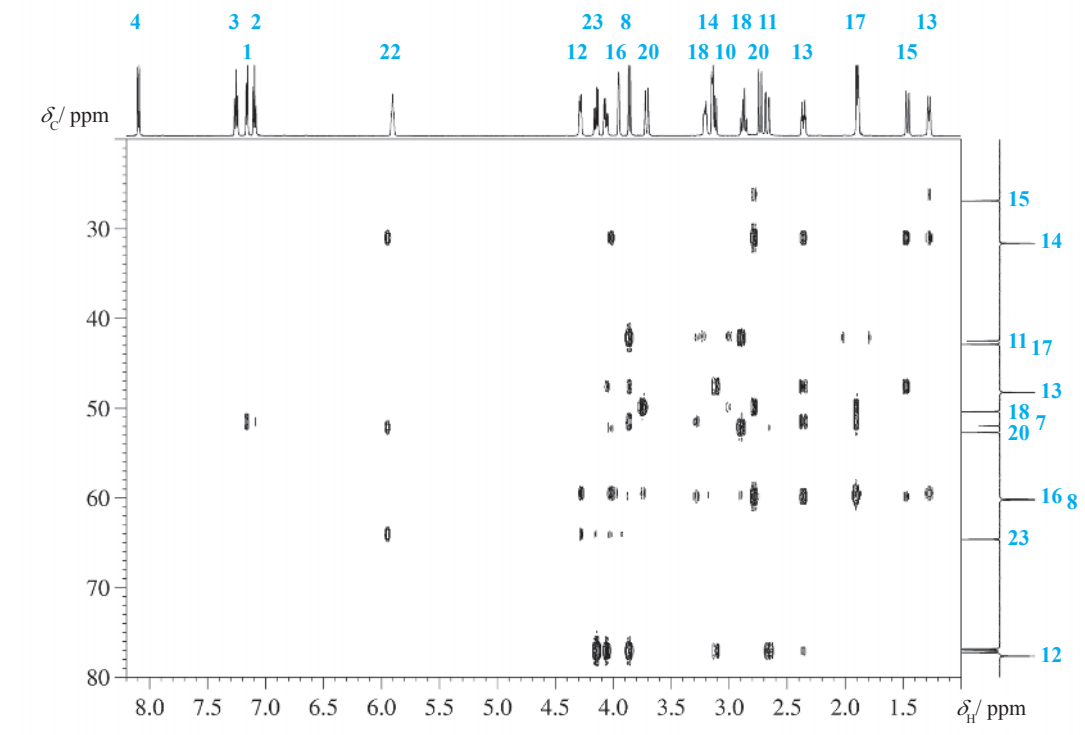

Fig. 1.6-2: HMBC expansion in the aliphatic ^{13}C region

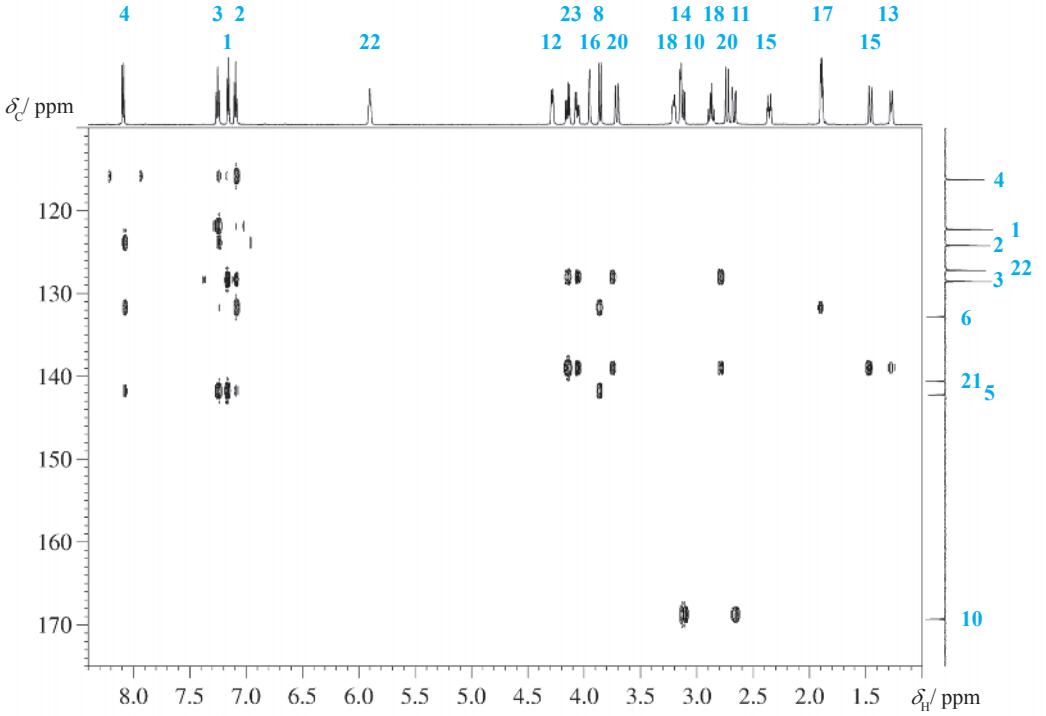

Fig. 1.6-3: HMBC expansion in the aromatic ^{13}C region

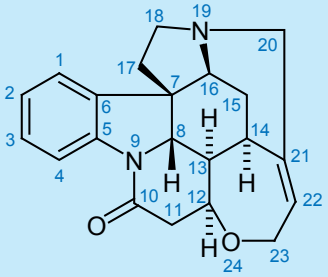

Scheme 1.6-3

8. Comments

HMBC has originally been derived from HMQC by simply increasing the delay after the first pulse before the creation of multiple-quantum coherence. The red-colored pulses in the sequence shown in Scheme 1.6-1 comprise this original experiment [1].

The first 90° proton pulse creates a transverse proton magnetization $-I_{H_y}$ as in Equation (1). During the delay d4 the ^2J and ^3J CH spin couplings develop and create antiphase magnetization $2I_{H_x}I_{C_z}$.

(1)

$$I_{Hz} + I_{Cz} \xrightarrow{I_{Hx}} -I_{Hy} + I_{Cz} \xrightarrow{\pi J \tau I_{Hz} I_{Cz}} 2I_{Hx} I_{Cz}$$

The two ^{13}C pulses p3 and p4 and the three gradient pulses g1 to g3 during the preparation period **p** serve as a dual-stage low-pass filter [7]. They eliminate the signals of protons experiencing a one-bond coupling ^1J(C,H). Therefore the action of these pulses is not considered in the POF description and in the coherence pathway diagram.

The third 90° ^{13}C pulse p5 transforms the antiphase magnetization of ^nJ(C,H) into double-quantum magnetization $2I_{H_x}I_{C_y}$ as in Equation (2).

(2)

$$2I_{H_x} I_{C_z} \xrightarrow{I_{C_x}} -2I_{H_x} I_{C_y}$$

In the evolution period **e** this term develops ^{13}C chemical shift as in Equation (3). Of course, ^{1}H chemical shift and H,H spin coupling also evolve during t_1. The former is removed by the 180° proton pulse p2, which for simplicity is not shown in the equations. Furthermore, this 180° proton pulse interchanges double-quantum and zero-quantum terms.

$$\xrightarrow{\Omega_C t_1 I_{C_z}} -2I_{H_x}I_{C_y}\cos\Omega_C t_1 + 2I_{H_x}I_{C_x}\sin\Omega_C t_1 \qquad \textbf{(3)}$$

In the mixing period **m** the adiabatic 180° refocusing pulse p6 in the ^{13}C channel, together with the pair of gradients g4 and g5 which are working in the echo-antiecho mode, selects for protons bound to ^{13}C only and suppresses all protons bound to ^{12}C. The final pulse p7 transfers the magnetization back to the proton channel as given in equation (4).

$$\xrightarrow{I_{C_x}} -2I_{H_x}I_{C_z}\cos\Omega_C t_1 + 2I_{H_x}I_{C_x}\sin\Omega_C t_1 \qquad \textbf{(4)}$$

In the detection period **d** the proton chemical shifts are sampled without ^{13}C decoupling. This is because despite the low-pass filter, some correlation signals via ^{1}J(C,H) can be seen in any HMBC spectrum. In order to distinguish these signals from the desired correlations it is advisable not to use ^{13}C decoupling, so ^{1}J breakthrough, giving rise to large doublets.

[1] A. Bax, M. F. Summers "^{1}H and ^{13}C assignments from sensitivity-enhanced detection of heteronuclear multiple-bond connectivity by multiple quantum NMR" *J. Am. Chem. Soc.* **1986**, *108*, 2093–2094.

[2] W. Willker, D. Leibfritz, R. Kerssebaum, W. Bermel "Gradient selection in inverse heteronuclear correlation spectroscopy" *Magn. Reson. Chem.* **1993**, *31*, 287–292.

[3] J. Ruiz-Cabello, G. W. Vuister, C. T. W. Moonen, P. van Gelderen, J. S. Cohen, P. C. M. van Zijl "Gradient-enhanced heteronuclear correlation spectroscopy. Theory and experimental aspects" *J. Magn. Reson.* **1992**, *100*, 282–302.

[4] R. Araya-Maturana, T. DelgadoCastro, W. Cardona, B. E. Weiss-Lopez "Use of long-range C-H heteronuclear multiple bond connectivity in the assignment of the ^{13}C NMR spectra of complex organic molecules" *Current Organic Chemistry*, **2001**, *5*, 253–263.

[5] W. F. Reynolds, R. G. Enríquez, "Choosing the best pulse sequences, acquisition parameters, postacquisition processing strategies, and probes for natural product structure elucidation by NMR spectroscopy" *J. Nat. Prod.* **2002**, *65*, 221–244.

[6] D. O. Cicero, G. Barbato, R. Bazzo, "Sensitivity enhancement of a two-dimensional experiment for the measurement of heteronuclear long-range coupling constants, by a new scheme of coherence selection by gradients" *J. Magn. Reson.* **2001**, *148*, 209–213.

[7] A. Meissner, O. W. Sørensen, "Measurement of J(H,H) and long-range *J*(X,H) coupling constants in small molecules, broadband XLOC and *J*-HMBC" *Magn. Reson. Chem*. **2001**, *39*, 49–52.

[8] R. Wagner, S. Berger, "ACCORD-HMBC: A superior technique for structural elucidation" *Magn. Reson. Chem*. **1998**, *36*, S44–S46.

[9] R. Burger, C. Schorn, P. Bigler, "HMSC: Simultaneously detected heteronuclear shift correlation through multiple and single bonds" *J. Magn. Reson.* **2001**, *148*, 88–94.

[10] N. T. Nyberg, J. O. Duus, O. W. Soerensen, "Editing of H2BC NMR spectra" *Magn. Reson. Chem.* **2005**, *43*, 971–974.

[11] T. E. Burrow, P. G. Enriquez, W. F. Reynolds "The signal/noise of an HMBC spectrum can depend dramatically upon the choice of acquisition and processing parameters" *Magn. Reson. Chem*. **2009**, *47*, 1086–1094.

[12] W. Schoefberger, J. Schlagnitweit, N. Müller "Recent developments in heteronuclear multiple-bond correlation experiments" *Ann. Rep. NMR Spectrosc*. **2011**, *72*, 1−60.

8. Questions

A. Why is HMBC intrinsically less sensitive than HSQC?

B. What is the expected range of ^{1}J(C,H) in organic Chemistry?

C. Why does one observe ^{1}J breakthrough especially for C-4 and C-17?

D. Why has the processing of this spectrum to use the magnitude mode, although the phase-sensitive echo-antiecho recording technique is employed?

E. Explain in detail how the gradient supported dual-stage low-pass filter functions.

F. Calculate the gradient strength for g4 and g5 in the case of ^{1}H, ^{15}N HMBC.

G. Why is an adiabatic chirp pulse used for p6?

9. Own Observations